

Wave packet dynamics in 2DEG with spin orbit coupling: splitting and *zitterbewegung*

V. Ya. Demikhovskii, G. M. Maksimova and E. V. Frolova*
Nizhny Novgorod State University,
Gagarin Ave., 23, Nizhny Novgorod 603950, Russian Federation
(Dated: today)

We study the effect of splitting and *zitterbewegung* of 1D and 2D electron wave packets in the semiconductor quantum well under the influence of the Rashba spin orbit coupling. Results of our investigations show that the spin orbit interaction induces dramatic qualitative changes in the evolution of spin polarized wave packet. The initial wave packet splits into two parts with different spin polarization propagating with unequal group velocity. This splitting appears due to the presence of two branches of electron spectrum corresponding to the stationary states with different chirality. It is demonstrated also that in the presence of external magnetic field \mathbf{B} perpendicular to the electron gas plane the wave packet splits into two parts which rotates with different cyclotron frequencies. It was shown that after some periods the electron density distributes around cyclotron orbit and the motion acquire an irregular character. Our calculations were made for both cases of weak and strong spin orbit coupling.

PACS numbers: 73.21.Hb, 71.10.Pm, 72.10.-d, 73.23.-b

I. INTRODUCTION

Producing and detecting spin polarized currents in semiconductor nonmagnetic devices is the ultimate goal of spintronics. The intrinsic spin orbit interaction¹ existing in low dimensional systems which couples electron momentum to its spin is one of the most promising tools for realizing spin polarized transport. For this reasons, during the last years a substantial amount of work has been devoted to study effects of spin orbit interaction on the transport properties of nanostructures (for a review, see, e. g.^{2,3,4}).

At first time the electron wave packet dynamics including the problem of *zitterbewegung* in semiconductor quantum well under the influence of the spin orbit Rashba and Dresselhaus coupling has been considered by Schliemann, Loss and Westervelt⁵. In this work the oscillatory motion of the electron wave packets reminiscent of the *zitterbewegung* of relativistic electrons was studied for free electron motion i.e., in the absence of electric or magnetic field. The authors of⁵ predicted the resonance amplification of *zitterbewegung* oscillations for the electron moving in a quantum wire with parabolic confinement potential and propose to observe this fundamental phenomena experimentally using high resolution scanning probe microscopy imaging techniques.

The *zitterbewegung* of the heavy and light holes in 3D semiconductors was investigated in⁶. In this paper the semiclassical motion of holes in the presence of a constant electric field was studied by numerical solution of the Heisenberg equations for momentum and spin operators in the Luttinger model of spectrum. It was shown that the hole semiclassical trajectories contain rapid small amplitude oscillations reminiscent the *zitterbewegung* of relativistic electrons. It should be noted, however, that the spatial structure of the wave packet and the changing of its shape due to effect of splitting in^{5,6} was not considered.

At the same time the splitting of spin polarized electron beams in the systems with spin orbit coupling was investigated in a series of works. In particular, the authors of papers^{7,8} propose to use the lateral interface between two regions in gated two-dimensional heterostructure with different strength of spin orbit coupling to polarize the electron. They have shown theoretically that in this structure a beam with a nonzero angle of incidence splits into some spin polarization components propagating at different angles. The similar effect of electron spin-polarized reflection in heterostructures and spatial separation of the electron beams after reflection has been observed experimentally in⁹.

The transverse electron focusing in systems with spin orbit coupling at the presence of perpendicular magnetic field was theoretically analyzed in¹⁰ where it was shown that in the weak magnetic field regime and for a given energy, the two branches of states have different cyclotron radii. The effect of spatial separation of the electron trajectories of different spin states in a perpendicular magnetic field has been experimentally observed in¹¹.

In this work we study the striking dynamics of the electron wave packets in a narrow A_3B_5 quantum well at the presence of the spin orbit k -linear Rashba coupling, which arise due to structural inversion ("up-down") asymmetry. The splitting of the wave packets in two parts appear due to the presence of the electron states with "plus" and "minus" chirality, which propagate with different group velocity. These two parts of the split packet can be characterized by different spin density. It is found that electron trajectories contain small amplitude damped oscillation. We show that the packet splitting leads to the damping of *zitterbewegung*. The splitting and *zitterbewegung* of wave packet is naturally accompanied by its broadening due to effect of dispersion.

We investigate also the atypical cyclotron dynamics of the wave packet in a perpendicular magnetic field. It was shown that due to the spin orbit coupling the packet

with spin parallel to the magnetic field splits into two parts which rotate with different cyclotron frequencies. We determine the moments when two parts of the packet are located at opposite points of the cyclotron orbit and after that they return many times back to their initial state. With the time due to the incommensurability of the cyclotron frequencies and the ordinary packet broadening the electron density distributes randomly around the cyclotron orbit. All our calculations were made for the material parameters of the real semiconductor structures with a relatively strong and weak spin orbit and Zeeman interaction.

The paper is organized as follows. In Sec. II we introduce the Green functions for two dimensional electrons in the presence of Rashba spin orbit interaction and analyze the evolution of 1D wave packet. The analytical and numerical results illustrate the effects of packet splitting and *zitterbewegung*. In section III we describe in details the time development of the 2D wave packets. Finally, in Sec. IV we discuss the manifestation of the spin orbit interaction in the evolution of coherent wave packet in a magnetic field perpendicular to electron gas plane. The splitting of the initial coherent packet and distribution electron probability via cyclotron orbit is considered. Section V concludes with a discussion of the results. The Appendix provides the mathematical details necessary to obtain Eqs. (36a) and (36b).

II. THE DYNAMIC OF THE ONE-DIMENSIONAL WAVE PACKETS

In this section we consider the specific character of the wave packet dynamics in the systems with Rashba spin orbit coupling¹. The Hamiltonian of the system under consideration reads

$$H = H_0 + H_R = \frac{\mathbf{p}^2}{2m} + \alpha(\hat{p}_y\hat{\sigma}_x - \hat{p}_x\hat{\sigma}_y), \quad (1)$$

where $\mathbf{p} = -i\hbar\nabla$ is the momentum operator, m is the electron effective mass, α is the Rashba coupling constant, and the components of the vector σ denotes the spin Pauli matrices. The eigenfunctions for the in-plane motion identified by the quantum numbers $\mathbf{p}(p_x, p_y)$ are

$$\phi_{\mathbf{p},s}(\mathbf{r}) = \frac{1}{2\sqrt{2\pi\hbar}} e^{i\mathbf{p}\mathbf{r}} \begin{pmatrix} 1 \\ -ise^{i\varphi} \end{pmatrix}, \quad (2)$$

Here φ is the angle between the electron momentum \mathbf{p} and x axis, so $e^{i\varphi} = \frac{p_x + ip_y}{p}$, $s = \pm 1$ denotes the branch index. The energy spectrum of the Hamiltonian (1) corresponding to two branches has the form

$$\varepsilon_{\pm}(p) = \frac{p^2}{2m} \pm \alpha p, \quad (3)$$

where $p = \sqrt{p_x^2 + p_y^2}$. Using the definition $\hat{\mathbf{v}} = \frac{d\mathbf{r}}{dt} = \frac{i}{\hbar}[H, \mathbf{r}]$, one can obtain from Eq.(1) the velocity operator

components

$$\hat{v}_x = \frac{p_x}{m} - \alpha\sigma_y, \quad \hat{v}_y = \frac{p_y}{m} + \alpha\sigma_x. \quad (4)$$

To analyze the time evolution of electron the initial states we use the Green's function of the nonstationary equation, which is a non diagonal 2×2 matrix

$$G_{ik} = \begin{pmatrix} G_{11} & G_{12} \\ G_{21} & G_{22} \end{pmatrix}. \quad (5)$$

Here $i, k = 1, 2$ are matrix indexes and matrix elements can be written as an integrals

$$G_{ik}(\mathbf{r}, \mathbf{r}', t) = \sum_s \int d\mathbf{p} \phi_{\mathbf{p},s,i}(\mathbf{r}, t) \phi_{\mathbf{p},s,k}^*(\mathbf{r}', 0). \quad (6)$$

In the present section we examine in details the dynamics of the quasi-1D wave packet in 2D system with spin orbit coupling. This problem allows the analytical solution. Let at the initial time $t = 0$ wave function to be a plane wave with wave number p_{0x} modulated by a Gaussian profile and spin polarized along the z direction

$$\begin{aligned} \Psi(\mathbf{r}, 0) &= \Psi(x, 0) = C \exp\left(-\frac{x^2}{2d^2} + ip_{0x}x/\hbar\right) \begin{pmatrix} 1 \\ 0 \end{pmatrix} = \\ &= f(x) \begin{pmatrix} 1 \\ 0 \end{pmatrix}, \end{aligned} \quad (7)$$

where coefficient C is equal to $(\frac{1}{dL_y\sqrt{\pi}})^{1/2}$, L_y is the size of the system in the y direction. The variance of the position operator $\langle (\Delta x)^2 \rangle$ in this case is equal to $d^2/2$ and the variance $\langle (\Delta y)^2 \rangle$ exceed this value. The variance of the momentum operator p_x is $\langle (\Delta p_x)^2 \rangle = \hbar^2/2d^2$, and the average $\hat{\mathbf{p}}$ is equal to p_{0x} . One may consider the initial wave function as the limiting case of a 2D packet with the width along y direction much greater than along x i.e., $L_y \gg d$.

The electron wave function at any arbitrary moment of time can be found with the help of the Green's function

$$\begin{pmatrix} \Psi_1(x, t) \\ \Psi_2(x, t) \end{pmatrix} = \int dx' dy' \begin{pmatrix} G_{11}f(x') \\ G_{21}f(x') \end{pmatrix}, \quad (8)$$

where matrix elements G_{11} and G_{21} of the matrix (5) are determined by Eqs.(2),(3) and (6)

$$\begin{aligned} G_{11}(\mathbf{r}, \mathbf{r}', t) &= \frac{1}{(2\pi\hbar)^2} \int \exp\left(-\frac{ip^2t}{2m\hbar} + i\frac{\mathbf{p}(\mathbf{r}-\mathbf{r}')}{\hbar}\right) \times \\ &\times \cos\left(\frac{\alpha pt}{\hbar}\right) d\mathbf{p}, \end{aligned} \quad (9)$$

$$\begin{aligned} G_{21}(\mathbf{r}, \mathbf{r}', t) &= \frac{1}{(2\pi\hbar)^2} \int \exp\left(-\frac{ip^2t}{2m\hbar} + i\frac{\mathbf{p}(\mathbf{r}-\mathbf{r}')}{\hbar}\right) \times \\ &\times \sin\left(\frac{\alpha pt}{\hbar}\right) \frac{p_x + ip_y}{p} d\mathbf{p}. \end{aligned} \quad (10)$$

By using the formula

$$e^{iq \cos \psi} = J_0(q) + 2 \sum_{n=1} J_{2n}(q) \cos(2n\psi) + 2i \sum_{n=1} J_{2n-1}(q) \sin((2n-1)\psi). \quad (11)$$

and by integrating over the angle variable in Eqs.(9), (10) we finally have

$$G_{11} = \frac{1}{2\pi\hbar^2} \int_0^\infty \exp(-i\frac{p^2 t}{2m\hbar}) J_0\left(\frac{p|\mathbf{r}-\mathbf{r}'|}{\hbar}\right) \times \cos\left(\frac{\alpha p t}{\hbar}\right) p dp, \quad (12)$$

$$G_{21} = \frac{(x-x') + i(y-y')}{2\pi\hbar^2 |\mathbf{r}-\mathbf{r}'|} \int_0^\infty \exp(-i\frac{p^2 t}{2m\hbar}) \times J_1\left(\frac{p|\mathbf{r}-\mathbf{r}'|}{\hbar}\right) \sin\left(\frac{\alpha p t}{\hbar}\right) p dp, \quad (13)$$

where J_0 and J_1 are Bessel functions. Substituting Eqs. (12), (13) and (7) into Eq.(8) and integrating over x' and y' , we find the analytical expression for the spinor components $\psi_{1,2}(x, t)$. It should be noted that two electron bands with chirality "plus" and "minus" give different contribution to the electron wave functions. The calculation of the expressions for $\Psi_{1,2}$ leads to the following electron probability densities $|\Psi_1|^2$ and $|\Psi_2|^2$ at any arbitrary moment of the time

$$|\Psi_1|^2 = \frac{C^2}{\sqrt{1+\gamma^2 t^2}} \left[\exp\left(-\frac{(x+(\alpha-\hbar k_0/m)t)^2}{d^2(1+\gamma^2 t^2)}\right) + \exp\left(-\frac{(x-(\alpha+\hbar k_0/m)t)^2}{d^2(1+\gamma^2 t^2)}\right) + 2 \exp\left(-\frac{(x+(\alpha-\hbar k_0/m)t)^2}{2d^2(1+\gamma^2 t^2)}\right) + \frac{(x-(\alpha+\hbar k_0/m)t)^2}{2d^2(1+\gamma^2 t^2)} \right] \times \cos\left(\frac{2(k_0 d^2 + \gamma t x) \alpha t}{d^2(1+\gamma^2 t^2)}\right), \quad (14a)$$

$$|\Psi_2|^2 = \frac{C^2}{\sqrt{1+\gamma^2 t^2}} \left[\exp\left(-\frac{(x+(\alpha-\hbar k_0/m)t)^2}{d^2(1+\gamma^2 t^2)}\right) + \exp\left(-\frac{(x-(\alpha+\hbar k_0/m)t)^2}{d^2(1+\gamma^2 t^2)}\right) - 2 \exp\left(-\frac{(x+(\alpha-\hbar k_0/m)t)^2}{2d^2(1+\gamma^2 t^2)}\right) + \frac{(x-(\alpha+\hbar k_0/m)t)^2}{2d^2(1+\gamma^2 t^2)} \right] \times$$

$$\times \cos\left(\frac{2(k_0 d^2 + \gamma t x) \alpha t}{d^2(1+\gamma^2 t^2)}\right), \quad (14b)$$

where $\gamma = \hbar/d^2 m$ is the inverse broadening time $p_{0x} = \hbar k_0$.

As follows from Eqs.(14a), (14b) the shape of the function $\rho(x, t)$ essentially depends on the parameter $\eta = \frac{m^2 \alpha^2 d^2}{\hbar^2}$. In the case wide packet when the momentum variance is much more $(m\alpha)^2$ and the inequality $\eta \ll 1$ takes place, the evolution looks like at the absence of Rashba term. Otherwise when $\eta \gg 1$ the initial wave packet splits into two parts which propagate with different group velocity, so the distance between these two parts increases linear in time. This two parts correspond to the first and second terms in square brackets in Eq.(14a) and Eq.(14b). The third terms in Eq.(14a), (14b) describe the oscillation of the components of electron density $|\Psi_1|^2$ and $|\Psi_2|^2$ in the region of the overlapping of two split parts of the packet. It is clear that these oscillations originates from the interference between the states of different spectrum branches. When two parts of the packet move away from each other the amplitude of the oscillations decreases. The period of these oscillations along the x direction depends on the initial width of the packet d and equals to $\Delta x = \pi d^2(1+\gamma^2 t^2)/\alpha \gamma t^2$. So, if inequality $\gamma t \ll 1$ takes place the period of oscillation decreases with time and equals to $\Delta x = \pi m d^4 / \alpha \hbar t^2$ and when $\gamma t \gg 1$ the oscillation period is not depend on the time $\Delta x = \pi \hbar / m \alpha$.

To illustrate the evolution of the electron probability density $\rho(x, y) = |\Psi_1|^2 + |\Psi_2|^2$ we plot this function using Eq.(14a), (14b) at the Fig.1(a) for the moments of the time: $t = 0, t = 1, 5, t = 7$ (in the units of $\tau_0 = \gamma^{-1}$). The calculations was made for the parameters *GaAs/InGaAs* electron system: $m = 0,05m_0$, $\alpha = 3,6 \cdot 10^6 \text{ cm}\cdot\text{sec}^{-1}$ and the packet parameters: $d = 10^{-5} \text{ cm}$, $k_0 = 2,5 \cdot 10^5 \text{ cm}^{-1}$. Here one can clearly see that initial Gaussian wave packet Eq.(7) splits up at $t > 0$ into two parts propagating along the x direction. The width of each part of the packet increases in time as for the case of free particle.

To analyze spin dynamics one can consider the time evolution of the spin density

$$s_i(x, y, t) = \frac{\hbar}{2} (\Psi_1^*, \Psi_2^*) \hat{\sigma}_i \begin{pmatrix} \Psi_1 \\ \Psi_2 \end{pmatrix}, \quad (15)$$

Using Eqs.(14a) and (14b) we immediately find the expression for spin density $s_z = \frac{\hbar}{2} (|\Psi_1(\mathbf{r}, t)|^2 - |\Psi_2(\mathbf{r}, t)|^2)$, which demonstrate the oscillatory behavior as a function of x (see Fig.1(b)). The period of oscillation here is the same as for the functions $|\Psi_{1,2}(x, t)|$. For the spin density $s_y(x, t)$ the following result can be obtained

$$s_y(x, t) = \frac{\hbar}{\sqrt{\pi} L_y d \sqrt{1+\gamma^2 t^2}} \times \left[\exp\left(-\frac{(x-(\hbar k_0/m-\alpha)t)^2}{d^2(1+\gamma^2 t^2)}\right) - \right]$$

$$\left. - \exp\left(-\frac{(x - (\hbar k_0/m + \alpha)t)^2}{d^2(1 + \gamma^2 t^2)}\right) \right], \quad (16)$$

According to this equation both parts of the initial wave packet moving along the x direction with different velocities are characterized by the opposite spin orientation (at the same time the average spin component $\bar{S}_y = \int s_y(x, t) d\mathbf{r}$ is equal to zero).

Note that the components of wave function depend only on coordinate x , that leads to $\bar{p}_y = p_y = 0$, however the velocity $\bar{v}_y(t) \neq 0$. Really, using the definition Eq.(4) it is not difficult to obtain

$$\begin{aligned} \bar{v}_x(t) &= \frac{\hbar k_0}{m}, \\ \bar{v}_y(t) &= -\alpha \sin(2k_0 \alpha t) \exp\left(-\left(\frac{\alpha t}{d}\right)^2\right). \end{aligned} \quad (17)$$

As follows from these equations the average \bar{v}_y velocity performs the oscillations in the transverse direction (*zitterbewegung* or jittering) with the frequency $2k_0\alpha$ and the damping time is determined by the parameter d/α .

III. EVOLUTION OF TWO DIMENSIONAL PACKETS AT THE PRESENCE OF SPIN ORBIT COUPLING

We consider now the evolution of two dimensional wave packet at the presence of spin orbit coupling. Let us consider the following form of the Gaussian packet at the initial moment $t = 0$:

$$\begin{aligned} \Psi(\mathbf{r}, 0) &= C \exp\left(-\frac{r^2}{2d^2} + ip_{0x}x/\hbar\right) \begin{pmatrix} 1 \\ 0 \end{pmatrix} = \\ &= f(\mathbf{r}) \begin{pmatrix} 1 \\ 0 \end{pmatrix}, \end{aligned} \quad (18)$$

where $p_{0x} = \hbar k_0$ is the average momentum and $C = 1/\sqrt{\pi}d$. Then, using a Green's function method we arrive after some algebra at the following equations for the components of spinor (in the momentum space)

$$\begin{aligned} C_1(\mathbf{p}, t) &= \frac{d}{\sqrt{\pi}\hbar} \cos\left(\frac{\alpha p t}{\hbar}\right) \exp\left(-\frac{ip^2 t}{2m\hbar} - \right. \\ &\quad \left. -\frac{p^2 d^2}{2\hbar^2} - \frac{k_0^2 d^2}{2} + \frac{p_x k_0 d^2}{\hbar}\right), \end{aligned} \quad (19a)$$

$$\begin{aligned} C_2(\mathbf{p}, t) &= -\frac{d}{\sqrt{\pi}\hbar} \frac{p_x + ip_y}{p} \sin\left(\frac{\alpha p t}{\hbar}\right) \exp\left(-\frac{ip^2 t}{2m\hbar} - \right. \\ &\quad \left. -\frac{p^2 d^2}{2\hbar^2} - \frac{k_0^2 d^2}{2} + \frac{p_x k_0 d^2}{\hbar}\right), \end{aligned} \quad (19b)$$

After that $\Psi_{1,2}(\mathbf{r}, t)$ can be obtained directly by 2D Fourier transform of $C_{1,2}(\mathbf{r}, t)$:

$$\Psi_1(\mathbf{r}, t) = \frac{d}{\sqrt{\pi}} \int_0^\infty \exp\left(-i\frac{q^2 \hbar t}{2m} - \frac{q^2 d^2}{2} - \frac{k_0^2 d^2}{2}\right) \times$$

$$\begin{aligned} &\times I_0(q\sqrt{k_0^2 d^4 - r^2 + 2ik_0 d^2 r \cos \varphi}) \times \\ &\times \cos(\alpha q t) q d q, \end{aligned} \quad (20a)$$

$$\begin{aligned} \Psi_2(\mathbf{r}, t) &= -\frac{id}{\sqrt{\pi}} \frac{r \cos \varphi + ir \sin \varphi - ik_0 d^2}{\sqrt{r^2 - k_0^2 d^4 - 2ik_0 d^2 r \cos \varphi}} \times \\ &\times \int_0^\infty \exp\left(-i\frac{q^2 \hbar t}{2m} - \frac{q^2 d^2}{2} - \frac{k_0^2 d^2}{2}\right) \times \\ &\times J_1\left(\sqrt{r^2 - k_0^2 d^4 - 2ik_0 d^2 r \cos \varphi}\right) \times \\ &\times \sin(\alpha q t) q d q, \end{aligned} \quad (20b)$$

where J_1 and I_0 are the Bessel and the modified Bessel functions of the first and the zeroth order, φ is azimuthal angle in the xy plane. These expressions become simpler if the average momentum of a wave packet is equal to zero, i.e. $p_{0x} = 0$. In this case

$$\begin{aligned} \Psi_1 &= \frac{d}{\sqrt{\pi}} \int_0^\infty q J_0(qr) \cos(\alpha q t) \times \\ &\times \exp\left(-i\frac{q^2 \hbar t}{2m} - \frac{q^2 d^2}{2}\right) dq, \end{aligned} \quad (21a)$$

$$\begin{aligned} \Psi_2 &= \frac{d}{\sqrt{\pi}} \frac{y - ix}{r} \int_0^\infty q J_1(qr) \sin(\alpha q t) \times \\ &\times \exp\left(-i\frac{q^2 \hbar t}{2m} - \frac{q^2 d^2}{2}\right) dq. \end{aligned} \quad (21b)$$

As in the case of 1D packet the shape of the full electron density $\rho(x, t) = |\Psi_1|^2 + |\Psi_2|^2$ at $t > 0$ depends on the parameter $\eta = \frac{m^2 \alpha^2 d^2}{\hbar^2}$. In Fig. 2. we show the electron density $\rho(x, t)$ for the case $p_{0x} = 0$ at the time $t = 5$ (in the units of $\frac{d}{\alpha}$) and $\eta = 2, 7$. As one can see the spin-orbit coupling qualitatively change the character of the wave packet evolution, so that during the time the initial Gaussian packet turns into two axially symmetric parts. As follows from our analytical and numerical calculation the outer part propagates with group velocity which is greater than α and the inner part moves with group velocity lower than α . If $\eta \ll 1$, i.e. the packet is narrow enough, its evolution remained the standard broadening of the Gaussian packet of free particle.

In Fig. 3(a) it is shown the packet evolution for the case $\bar{p}_{0x} = \hbar k_0 \neq 0$. It is clear that in this case the cylindrical symmetry is absent, and two maximums of the electron density spread along the x direction with not equal velocities. Each one of these two parts are spin polarized. Fig. 3(b) illustrates the distribution of the spin polarization $s_y(x, y, t)$ for the initial state, polarized along z axis, Eq.(18). It is a smooth function which has different sign in the regions for two maximums of the electron density.

When $\bar{p}_x \neq 0$ the motion of the wave packet center along x accompanied by the oscillation of the packet center in a perpendicular direction, or *zitterbewegung*. Below we consider the effect of damping of *zitterbewegung* oscillation for 2D packet which was not predicted in⁷.

Using Eq.(22a) and Eq.(22b) we calculate the average value of the operator $\hat{y} = i\hbar \frac{\partial}{\partial p_y}$ and obtain for $t > 0$ the result

$$\begin{aligned} \bar{y}(t) = & -\frac{2d^2}{\hbar} \exp[-(k_0d)^2] \int_0^\infty \sin^2\left(\frac{\alpha pt}{\hbar}\right) \times \\ & \times \exp\left(-\frac{p^2d^2}{\hbar^2}\right) I_1\left(\frac{2pk_0d^2}{\hbar}\right) dp. \end{aligned} \quad (22)$$

In the case when wave packet is wide enough and the inequality $a = dk_0 \gg 1$ takes place, one can obtain a simple asymptotic formula for $\bar{y}(t)$. To show this we represent Eq. (22) as a sum of two terms

$$\begin{aligned} \bar{y}(t) = & -d \exp(-a^2) \left[\int_0^\infty \exp(-u^2) I_1(2au) du - \right. \\ & \left. - \int_0^\infty \cos\left(\frac{2\alpha tu}{d}\right) \exp(-u^2) I_1(2au) du \right] \\ = & -d \exp(-a^2) \left[\frac{1}{2a} (\exp(a^2) - 1) - Z \right], \end{aligned} \quad (23)$$

where we denote $\frac{pd}{\hbar} = u$, $Z = \text{Re}\left(\int_0^\infty \exp(-u^2 + i\frac{2\alpha tu}{d}) I_1(2au) du\right)$. To evaluate Z we replace the modified Bessel function $I_1(2dk_0u)$ by it's asymptotic formula $I_1(x) = \frac{e^x}{\sqrt{2\pi x}}$, which valid for the case $k_0d \gg 1$. After that the integral with respect to u can be evaluated using the stationary phase method that leads to the simple result

$$Z = \frac{1}{2kd} \exp\left(a^2 - \frac{\alpha^2 t^2}{d^2}\right) \cos(2\alpha k_0 t).$$

Substituting this expression into Eq.(23) we finally have

$$\bar{y}(t) = -\frac{1}{2k_0} \left[1 - \exp\left(-\frac{\alpha^2 t^2}{d^2}\right) \cos(2\alpha k_0 t) \right]. \quad (24)$$

The last result demonstrates clearly that $\bar{y}(t)$ experience the damped oscillations with the frequency $2\alpha k_0$ decaying for the time $\frac{d}{\alpha}$. In the real 2D structures the frequency of the *zitterbewegung* have the order of $10^{11} - 10^{12} \text{ sec}^{-1}$ for $k_0 \approx 10^{-5} - 10^{-6} \text{ cm}$. The amplitude of the *zitterbewegung* is proportional to the electron wavelength in x . At Fig. 4 we plot the function $\bar{y}(t)$ determined by Eq. (22) which demonstrates in accordance with Eq.(24) the effect of *zitterbewegung* damping. When $t \gg \frac{d}{\alpha}$ the oscillations stop and the center of the wave packet is shifts in direction perpendicular to the group

velocity at the value of $1/2k_0$. The last result coincides with⁷. Since the packet moves with constant velocity, the time oscillations of $\bar{y}(t)$ can be easily converted to the oscillation of the wave packet center in real x, y space.

IV. CYCLOTRON DYNAMICS OF 2D WAVE PACKET IN A PERPENDICULAR MAGNETIC FIELD

In this section we examine the cyclotron dynamics of electron wave packet rotating in a magnetic field $\mathbf{B}(0, 0, B)$ which is perpendicular to the plane of 2D electron gas. In this case the one-electron Hamiltonian including Rashba term reads

$$\begin{aligned} H = & \frac{(\hat{\mathbf{p}} + e\mathbf{A}/c)^2}{2m} + \alpha(\hat{\sigma}_y(\hat{p}_x + eA_y/c) - \hat{\sigma}_x\hat{p}_y) + \\ & + g\mu_B\sigma_z. \end{aligned} \quad (25)$$

Here e is the electron charge, m is the effective mass, $\hat{p}_{x,y}$ are the momentum operator components, α is the parameter of Rashba coupling, g is the Zeeman factor, and μ_B is the Bohr magneton. Bellow we use the Landau gauge for the vector potential $\mathbf{A} = (-By, 0, 0)$. Then the eigenvalues and the eigenfunctions of the Hamiltonian (25) indicating by quantum numbers $n, k_x, s = \pm 1$ and corresponding to two branches of levels can be evaluated analytically (see, e.g.,¹³)

$$E_n^\pm = \hbar\omega_c n \pm \left(E_0^2 + \frac{2n\alpha^2\hbar^2}{\ell_B^2} \right)^{1/2}, \quad (26)$$

where $E_0^+ = \frac{\hbar\omega_c}{2} - g\mu_B B$ is the zero Landau level, $n = 1, 2, 3, \dots$, $\omega_c = \frac{eB}{mc}$ is the cyclotron frequency, $\ell_B = \sqrt{\frac{\hbar}{m\omega_c}}$ is the magnetic length. The eigenspinors are

$$\begin{aligned} \psi_{n,k_x}^+ (\mathbf{r}) = & \frac{e^{ik_x x}}{\sqrt{2\pi A_n}} \begin{pmatrix} -iD_n \phi_{n-1}(y - y_c) \\ \phi_n(y - y_c) \end{pmatrix}, \\ \psi_{n,s}^- = & \frac{e^{ik_x x}}{\sqrt{2\pi A_n}} \begin{pmatrix} \phi_{n-1}(y - y_c) \\ -iD_n \phi_s(y - y_c) \end{pmatrix}, \\ \psi_0^+ = & \frac{e^{ik_x x}}{\sqrt{2\pi}} \begin{pmatrix} 0 \\ \phi_0(y - y_c) \end{pmatrix}. \end{aligned} \quad (27)$$

Here coefficients D_n are given by: $D_n = \frac{\sqrt{2n\alpha\hbar/\ell_B}}{E_0 + \sqrt{E_0^2 + 2n\alpha^2\hbar^2/\ell_B^2}}$, $A_n = 1 + D_n$, $\phi_m(y - y_c)$ are linear oscillator wave functions, $y_c = \ell_B^2 k_x$ is the center of oscillator. It should be noted that for enough weak magnetic field the dependence of energy E_n^- on quantum number n ($n \gg 1$) resembles the behavior of the function $\varepsilon_-(p)$, Eq. (3). Namely, for small n the values of energy E_n^+ are negative, decreasing with n , like for the hole states.

Using the Eqs.(26),(27) we can obtain components of the matrix Green's function which permits us to find the

time evolution of the initial state. The usual definition

$$G_{ij}(\mathbf{r}, \mathbf{r}', t) = \sum_{s=\pm} \int dk_x \times \sum_{n=0}^{\infty} \psi_{n,k_x,i}^s(\mathbf{r}, t) \psi_{n,k_x,j}^{*s}(\mathbf{r}, 0). \quad (28)$$

yields

$$G_{11}(\mathbf{r}, \mathbf{r}', t) = \frac{1}{2\pi} \int_{-\infty}^{+\infty} dk_x e^{ik_x(x-x')} \times \sum_{n=0}^{\infty} f_{n+1}(t) \phi_n(y-y_c) \phi_n(y'-y_c), \quad (29a)$$

$$G_{21}(\mathbf{r}, \mathbf{r}', t) = \frac{1}{2\pi} \int_{-\infty}^{+\infty} dk_x e^{ik_x(x-x')} \times \sum_{n=0}^{\infty} g_{n+1}(t) \phi_{n+1}(y-y_c) \phi_n(y'-y_c), \quad (29b)$$

where the time-dependent coefficients $f_n(t)$ and $g_n(t)$ are given by

$$f_n(t) = e^{-i\omega_c n t} (\cos \delta_n t - i(1 - \frac{2}{A_n}) \sin \delta_n t), \quad (30a)$$

$$g_n(t) = e^{-i\omega_c n t} \frac{2Dn}{A_n} \sin \delta_n t, \quad (30b)$$

and $\delta_n = \frac{1}{\hbar} \sqrt{E_0^2 + \frac{2n\alpha^2 \hbar^2}{\ell_B^2}}$.

Let the initial state coincides with the wave function of the coherent state in a magnetic field

$$\Psi(\mathbf{r}, 0) = \frac{1}{\sqrt{\pi} \ell_B} \exp(-\frac{r^2}{2\ell_B^2} + ip_{0x}x/\hbar) \begin{pmatrix} 1 \\ 0 \end{pmatrix}. \quad (31)$$

Such choice of wave function $\Psi(\mathbf{r}, 0)$ is motivated by the following: as it is well known, at the absence of spin orbit coupling the dynamics of coherent states in a magnetic field looks like the dynamics of a classical particle. To analyze the time evolution in our case one needs to calculate the wave function at $t > 0$. Straightforward algebra with using Eqs.(29a), (29b), (31) leads to the final expressions

$$\psi_1(\mathbf{r}, t) = \frac{1}{\sqrt{2\pi} \ell_B} \sum_{n=0}^{\infty} \frac{f_{n+1}(t)}{2^n n!} \int_{-\infty}^{+\infty} du e^{\varphi(x,y,u)} \times (-u)^n H_n(\frac{y}{\ell_B} - u), \quad (32a)$$

$$\psi_2(\mathbf{r}, t) = \frac{1}{2\pi \ell_B} \sum_{n=0}^{\infty} \frac{g_{n+1}(t)}{2^n n! \sqrt{n+1}} \int_{-\infty}^{+\infty} du e^{\varphi(x,y,u)} \times (-u)^n H_{n+1}(\frac{y}{\ell_B} - u), \quad (32b)$$

where $\varphi(x, y, u) = iu \frac{x}{\ell_B} - \frac{(p_{0x} \ell_B / \hbar - u)^2}{2} - \frac{u^2}{4} - \frac{y - u \ell_B}{2\ell_B}$.

The electron density obtained by numerical evaluations of the integrals Eqs.(32a) and (32b) is represented in Fig. 5 for relatively weak spin orbit coupling and strong magnetic field. The calculations was made for the material parameters of two dimensional *GaAs* heterostructure: $m = 0,067m_0$, $\alpha = 3,6 \cdot 10^5 \text{ cm} \cdot \text{sec}^{-1}$, $g = -0,44$, $B = 1T$ and $k_{0x} = p_{0x}/\hbar = 1,5 \cdot 10^6 \text{ cm}^{-1}$. It is not difficult to verify that the series in Eqs. (32a) and (32b) converge very rapidly as n increases. So for our parameters it suffices to take $n_{max} = 25$ to calculate the components $\psi_1(\mathbf{r}, t)$ and $\psi_2(\mathbf{r}, t)$. At $t > 0$ the initial wave packet (Fig. 5(a)) splits on two parts (Fig. 5(b)) which "rotate" with different incommensurable cyclotron frequencies. In accordance with Eqs.(26) these frequencies can be determine by the expressions

$$\omega_c^{\pm} = \frac{E_{n+1}^{\pm} - E_n^{\pm}}{\hbar} = \omega_c \pm \sqrt{E_0^2 + 2(n+1) \frac{\alpha^2 \hbar^2}{\ell_B^2}} \mp \sqrt{E_0^2 + 2n \frac{\alpha^2 \hbar^2}{\ell_B^2}}. \quad (33)$$

The effective n in this equation is connected with cyclotron radius via relation $R_c(t) = \frac{p_{0x}}{m\omega_c} = \sqrt{2n} \ell_B$. Believing that $\varsigma = \frac{2n\alpha^2 \hbar^2}{\ell_B^2 E_0^2} \ll 1$, i.e. in the case of a weak spin orbit coupling or strong magnetic field, one can obtain from (33) the approximate expression for the difference between cyclotron frequencies

$$\omega_c^+ - \omega_c^- = 2 \frac{\alpha^2 m}{E_0} \omega_c. \quad (34)$$

Fig.5(b) demonstrates for the case $\varsigma \ll 1$ the distribution of electron density at the moment when two parts are located at opposite points of the cyclotron orbit. The correspondent time can be determined from the relation $(\omega_c^+ - \omega_c^-)t_0 = \pi$ and hence for the *GaAs* structure we will have $t_0 = \frac{\pi}{\omega_c^+ - \omega_c^-} = \frac{\pi}{\omega_c} \frac{E_0}{2\alpha^2 m} = 45 \frac{2\pi}{\omega_c}$.

After some cyclotron periods two split packets merge again which is demonstrated in Fig.5(c). With time due to the effect of the broadening electron probability distributes randomly around cyclotron orbit that is shown in Fig.5(d).

In the opposite case of relatively strong spin orbit coupling or weak magnetic field when the inequality $\varsigma = \frac{2n\alpha^2 \hbar^2}{\ell_B^2 E_0^2} \gg 1$ holds true the difference between two cyclotron frequencies, as it follows from Eq.(33), equals to $\omega_c^+ - \omega_c^- = \frac{\sqrt{2}\alpha}{\sqrt{n} \ell_B}$. For the *InGaAs* structure with parameters $m = 0,05m_0$, $\alpha = 3,6 \cdot 10^6 \text{ cm} \cdot \text{sec}^{-1}$, $g = -10$, $B = 1T$ and $k_{0x} = p_{0x}/\hbar = 1,5 \cdot 10^6 \text{ cm}^{-1}$, we have $\varsigma = 8$ and the divergence time $t_0 \approx 2,3 \cdot \frac{2\pi}{\omega_c}$.

One can analyze the effects of the periodic splitting and reshaping of the wave packet in magnetic field as well as the process of distribution around cyclotron orbit by considering the time dependence of the cyclotron radius determined as $R(t) = \sqrt{\{\bar{x}(t)\}^2 + \{\bar{y}(t)\}^2}$. To do this we

represent the average value of coordinates $x_1 = x$, $x_2 = y$ as

$$\begin{aligned} \bar{x}_i &= \int \psi_1^*(\mathbf{r}, t) x_i \psi_1(\mathbf{r}, t) d\mathbf{r} + \\ &+ \int \psi_2^*(\mathbf{r}, t) x_i \psi_2(\mathbf{r}, t) d\mathbf{r}, \end{aligned} \quad (35)$$

where ψ_1 and ψ_2 are determined by Eqs. (32a) and (32b). The lengthy calculations (see the Appendix) eventually yield the explicit expression for the $\bar{x}(t)$ and $\bar{y}(t)$:

$$\begin{aligned} \bar{x}(t) &= -\frac{\ell_B}{3} \exp\left(-\frac{p_{0x}^2 \ell_B^2}{3\hbar^2}\right) \times \\ &\times \left\{ \cos \omega_c t \sum_{k=0} S_k(t) H_{2k+1} \left(i \sqrt{\frac{2}{3}} p_{0x} \ell_B / \hbar \right) + \right. \\ &\left. + \sin \omega_c t \sum_{k=0} P_k(t) H_{2k+1} \left(i \sqrt{\frac{2}{3}} p_{0x} \ell_B / \hbar \right) \right\}, \end{aligned} \quad (36a)$$

$$\begin{aligned} \bar{y}(t) &= q \ell_B^2 + \frac{\ell_B}{3} \exp\left(-\frac{p_{0x}^2 \ell_B^2}{3\hbar^2}\right) \times \\ &\times \left\{ \cos \omega_c t \sum_{k=0} P_k(t) H_{2k+1} \left(i \sqrt{\frac{2}{3}} p_{0x} \ell_B / \hbar \right) - \right. \\ &\left. - \sin \omega_c t \sum_{k=0} S_k(t) H_{2k+1} \left(i \sqrt{\frac{2}{3}} p_{0x} \ell_B / \hbar \right) \right\}. \end{aligned} \quad (36b)$$

As one can see, the dependence of $\bar{x}(t)$ and $\bar{y}(t)$ on the time are determined by both the factors $\cos \omega_c t$ and $\sin \omega_c t$ as well as by functions

$$\begin{aligned} S_k(t) &= i \frac{(-1)^k}{k!} \left(\frac{1}{12} \right)^k [\xi_{k+2} \cos \delta_{k+1} t \sin \delta_{k+2} t - \\ &- \xi_{k+1} \cos \delta_{k+2} t \sin \delta_{k+1} t], \end{aligned} \quad (37a)$$

$$\begin{aligned} P_k(t) &= i \frac{(-1)^k}{k!} \left(\frac{1}{12} \right)^k [\cos \delta_{k+1} t \cos \delta_{k+2} t + \\ &+ (\xi_{k+1} \xi_{k+2} + 4 \sqrt{\frac{k+2}{k+1}} \frac{D_{k+1} D_{k+2}}{A_{k+1} A_{k+2}}) \times \\ &\times \sin \delta_{k+1} t \cos \delta_{k+2} t], \end{aligned} \quad (37b)$$

$$\xi_k = \frac{D_k^2 - 1}{D_k^2 + 1},$$

which describe the additional time dependence due to spin precession. Note that the frequencies $\delta_k = \frac{1}{\hbar} \sqrt{E_0^2 + \frac{2k\alpha^2 \hbar^2}{\ell_B^2}}$ are incommensurable. As a check on this formalism, it is not difficult to show that in the absence of Rashba coupling ($\alpha = 0$) as it follows from Eqs. (36a) and (36b)

$$\begin{aligned} \bar{x}(t) &= p_{0x} \ell_B^2 / \hbar \sin \omega_c t, \\ \bar{y}(t) &= p_{0x} \ell_B^2 (1 - \cos \omega_c t), \end{aligned} \quad (38)$$

that correspond to the classical motion of charged particle in the magnetic field with a constant radius.

The time dependence of the cyclotron radius $R(t)$ in the system with Rashba is presented at Fig. 6. It is clear that the oscillations of $R(t)$ are connected with the effects of periodic splitting and reshaping of wave packets. The radius has the minimal values at the moments when two parts of the packet are located at the opposite point of cyclotron orbit. This situation is shown at FIG 5.(b). The first minimum labeled by the letter *b* at FIG .6 One can see that the time of the first minimum approximately coincides to our estimation made above: $t_0 \approx 45T_c$. The radius is maximal at the moments of the packet reshaping that is shown at Fig. 5(c) (two of these points labeled by the letters *a* and *c*. Due to the effects of incommensurability of the cyclotron frequencies and the packet broadening the amplitude of the oscillations decreases with the time After that the electron density distributes around cyclotron orbit, the amplitude of the oscillation ceases and the electron density distribution acquire the no regular character (Fig.5(d)).

We evaluate also the distribution of the electron density for the structure with relatively strong spin orbit coupling. For such systems instead of the repeated process of the splitting and restoring of the wave packet discussed above the transition to the irregular distribution along the cyclotron orbit can be realized for the time of the order of one cyclotron period. This conclusion is confirmed by the simple estimation made for the *InGaAs/GaAs* structure discussed above.

V. CONCLUSIONS

We have analyzed the evolution of 1D and 2D wave packets in 2D electron gas with linear Rashba spin orbit coupling. We showed that the electron packet dynamics differs drastically from usual quantum dynamics of electrons with parabolic energy spectrum. Depending on the initial spin polarization packet splits in two parts which propagate with different velocities and have different spin orientation. At the time when two parts of wave packet overlap, the packet center performs oscillations in much the same way as for a relativistic particle. The direction of these oscillations is perpendicular to the packet group velocity. When the distance between split parts exceeds the initial width of the packet these oscillations stop.

In the 2D semiconductor structures placed in a perpendicular magnetic field the spin orbit coupling changes the cyclotron dynamics of charged particles. As at the absence of magnetic field the initial packet splits in two parts, which rotate in a perpendicular magnetic field with different incommensurable cyclotron frequencies. As a result, after some cyclotron periods these parts join again. The corresponding time t_0 essentially depends upon the ratio of the energy of spin orbit coupling and the distance between Landau levels, Eq.(26): $\varsigma = \frac{2n\alpha^2 \hbar^2}{\ell_B^2 E_0^2}$. Thus, for the systems with weak and relatively strong

spin orbit coupling e.g. *GaAs* and *InGaAs* heterostructures, the time t_0 equals to $45T_c$ and $2, 3T_c$, respectively.

The splitting and *zitterbewegung* of the wave packets in nanostructures with spin-orbit coupling can be observed experimentally in low dimensional structures. In particular, these effects should determine the electron dynamics and high-frequency characteristics of the field effect transistor by Datta and Das¹³, and other spintronic devices. Simple estimations show that during the time of the wave packet propagation through the ballistic transistor channel where the distance between emitter and collector is of the order of $1\mu m$, the distance between two split parts of the wave packet becomes comparable with its initial size. In this situation the high-frequency characteristics of the field effect transistor should be substantially affected by the spin-orbit coupling. Moreover, the atypical semiclassical dynamics of a spin-orbit system placed in a magnetic field will influence the shape of the cyclotron resonance line in 2D systems with spin orbit coupling. An important feature of these experiments is that the electron transport is in the ballistic regime and thus the momentum relaxation time τ should be considered much more greater compared with the typical splitting time.

Acknowledgments

The authors are grateful to D.V. Khomitsky for useful discussions. This work was supported by the program of the Russian Ministry of Education and Science "Development of scientific potential of high education" (project 2.1.1.2363).

VI. APPENDIX

This appendix provides some of details involved in obtaining the average value of the position operator given by Eqs.(36a), (36b). According to Eq.(35)

$$\bar{y}(t) = \bar{y}_1(t) + \bar{y}_2(t). \quad (A.1)$$

Consider the calculation of the first term $\bar{y}_1(t)$. Using the initial wave function, Eq.(31), we obtain

$$\begin{aligned} \bar{y}_1(t) &= \int \int \frac{d\mathbf{r}' d\mathbf{r}''}{\pi \ell_B^2} \times \\ &\times \exp\left(-\frac{r'^2 + r''^2}{2\ell_B^2} + i\frac{p_{0x}(x' - x'')}{\hbar}\right) \times \\ &\times \int G_{11}(\mathbf{r}, \mathbf{r}', t) y G_{11}^*(\mathbf{r}, \mathbf{r}'', t) d\mathbf{r}. \end{aligned} \quad (A.2)$$

Denote the last integral in this equation as

$$M_{11}^y = \int G_{11}(\mathbf{r}, \mathbf{r}', t) y G_{11}^*(\mathbf{r}, \mathbf{r}'', t) d\mathbf{r}. \quad (A.3)$$

Then substituting Eq.(29a) into Eq.(A.3) and using the well known formula for a linear harmonic oscillator

functions

$$\begin{aligned} &\int_{-\infty}^{+\infty} y \phi_n(y - y_c) \phi_k(y - y_c) dy = \\ &= \frac{\ell_B}{\sqrt{2}} \left(\sqrt{n} \delta_{k, n-1} + \sqrt{n+1} \delta_{k, n+1} \right) + y_c \delta_{n, k}, \end{aligned} \quad (A.4)$$

we will have

$$M_{11}^y = \frac{1}{2\pi} \int_{-\infty}^{+\infty} e^{ik_x(x-x'')} \mu(y', y'', t, y_c) dk_x. \quad (A.5)$$

Here

$$\begin{aligned} \mu(y', y'', t, y_c) &= \frac{\ell_B}{\sqrt{2}} \times \\ &\times \left(\sum_{n=0} \sqrt{n} f_{n+1}(t) f_n^*(t) \phi_n(y' - y_c) \phi_{n-1}(y'' - y_c) + \right. \\ &\quad \left. + \sum_{n=0} \sqrt{n+1} f_{n+1}(t) f_{n+2}^*(t) \times \right. \\ &\quad \left. \times \phi_n(y' - y_c) \phi_{n+1}(y'' - y_c) \right) + \\ &\quad + y_c \sum_{n=0} |f_{n+1}(t)|^2 \phi_n(y' - y_c) \phi_n(y - y_c), \end{aligned} \quad (A.6)$$

where the coefficients $f_n(t)$ are given by Eq.(30a). We calculate $\bar{y}_1(t)$ by substituting Eqs.(A.5), (A.6) into (A.2). The resulting integrals can be evaluated by using Gaussian transformation¹⁴

$$\begin{aligned} \frac{1}{\sqrt{\pi}} \int_{-\infty}^{+\infty} e^{-(x-y)^2} H_n(y) dy &= (2x)^n, \\ \frac{1}{\sqrt{\pi}} \int_{-\infty}^{+\infty} e^{-(x-y)^2} y^n dy &= \frac{H_n(ix)}{(2i)^n}. \end{aligned} \quad (A.7)$$

Finally we obtain

$$\begin{aligned} \bar{y}_1(t) &= \frac{\ell_B}{6} \exp\left(-\frac{(p_{0x}\ell_B)^2}{3\hbar^2}\right) \times \\ &\times \sum_{k=0} \psi_k(t) H_{2k+1}(i\sqrt{2/3}p_{0x}\ell_B/\hbar), \end{aligned} \quad (A.8)$$

where

$$\begin{aligned} \psi_k(t) &= \frac{i}{k!} \left(-\frac{1}{12}\right)^k (f_{k+1}^*(t) f_{k+2}(t) + \\ &\quad + f_{k+1}(t) f_{k+2}^*(t) - 2|f_{k+1}(t)|^2). \end{aligned} \quad (A.9)$$

Performing the same kind of calculation we have for $\bar{y}_2(t)$:

$$\begin{aligned} \bar{y}_2(t) &= \frac{\ell_B}{6} \exp\left(-\frac{(p_{0x}\ell_B)^2}{3\hbar^2}\right) \times \\ &\times \sum_{k=0} \gamma_k(t) H_{2k+1}(i\sqrt{2/3}p_{0x}\ell_B/\hbar), \end{aligned} \quad (A.10)$$

where

$$\gamma_k(t) = \frac{i}{k!} \left(-\frac{1}{12} \right)^k (g_{k+1}^*(t)g_{k+2}(t) + g_{k+1}(t)g_{k+2}^*(t) - 2|g_{k+1}|^2), \quad (\text{A.11})$$

and the coefficients $f_k(t)$ and $g_k(t)$ in Eqs.(A.9), (A.11) are determined by Eqs.(30a), (30b). The preceding expressions immediately lead to the average value $\bar{y}(t)$ given in Eq. (36b). The evaluation of $\bar{x}(t)$ can be obtained by following the procedure similar to that which led to Eq.(36a).

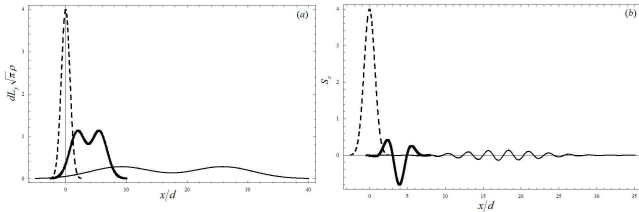


FIG. 1: The electron probability density $\rho(x,t) = |\Psi_1|^2 + |\Psi_2|^2$ (a), and spin density s_z (b). The dashed, thick and thin lines correspond to different moments of the time namely $t_1 = 0$, $t_2 = 1, 5$ and $t_3 = 7$ (in the units $\tau_0 = \gamma^{-1}$).

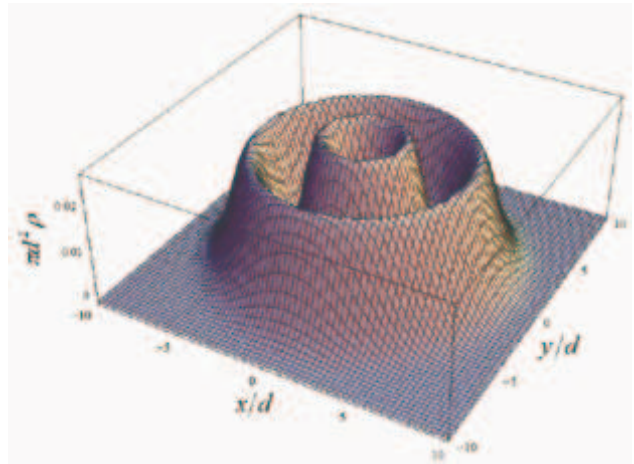


FIG. 2: (Color on line). The electron probability density $\rho(x,t) = |\Psi_1|^2 + |\Psi_2|^2$ for the initial state Gaussian packet Eq.(18) with $p_{0x} = 0$ at the time $t = 5$ (in the units d/α).

* Electronic address: demi@phys.unn.ru

¹ J. Shlieman, arXiv:cond-mat/0602330v2, 6 Apr 2006.

² H.-A. Engel *et al.*, arXiv: cond-mat/0603306v1, 10 Mar 2006.

³ I. Zutic *et al.*, Rev. Mod. Phys. **76**, 323 (2004).

⁴ Yu.A. Bychkov and E.I. Rashba, Pis'ma Zh. Exsp. Teor. Fiz. **39**, 66 (1984) [JETP Lett. **39**, 78 (1984)].

⁵ A. Shekhter, M. Khodas and A.M. Finkel'stein, Phys. Rev. Lett. **92**, 086602 (2004).

⁶ A. Shekhter, M. Khodas and A.M. Finkel'stein, Phys. Rev. B **71**, 125114 (2005).

⁷ H. Chen, J.J. Heremans, J.A. Peters, A.O. Govorov, N. Goel, S.J. Chung, and M.B. Santos, Appl. Phys. Lett. **86**, 032113 (2005).

⁸ Gonsalo Usaj and C.A. Balserio, Phys. Rev. B **70**, 041301(R) (2004).

⁹ L.P. Rokhinson, V. Larkina, Y.B. Lyanda-Geller, L.N. Pfeiffer, and K.W. West, Phys. Rev. Lett. **93**, 146601 (2004).

¹⁰ J. Schliemann, D. Loss and R.M. Westervelt, Phys. Rev. Lett. **94**, 206801(2005).

¹¹ Z.F. Jiang *et al.*, Phys. Rev. B **72**, 045201(2005).

¹² S. Datta and B. Das, Appl. Phys. Lett. **56**, 665 (1990).

¹³ X.F. Wang and P. Vasilopoulos, Phys. Rev. B **67**, 085313(2003).

¹⁴ I.S. Gradshteyn and I.M. Ryzhik, *Tables of integrals, Series and Products* (Academic Press, New York, 1980).

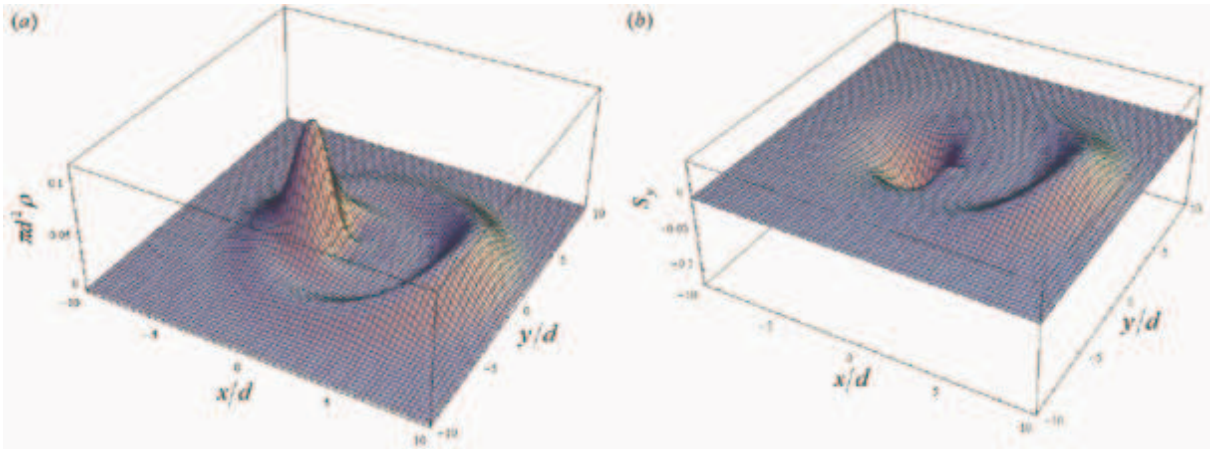


FIG. 3: (Color on line). Electron density $\rho(x, t) = |\Psi_1|^2 + |\Psi_2|^2$ (a) and spin density $s_z(x, y, t)$ (b) for $k_0 d = 1$ at the moment $t = 5$ (in units d/α).

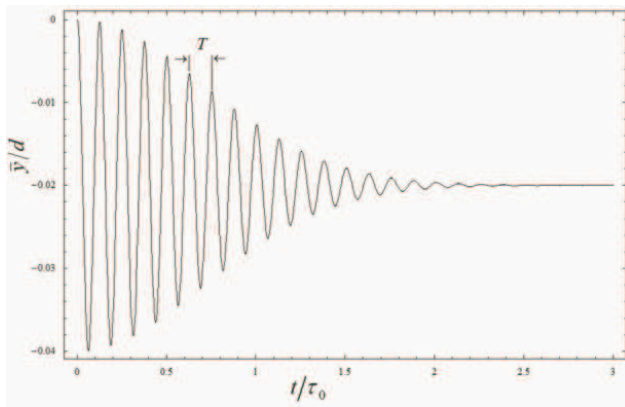


FIG. 4: The average coordinate of $\bar{y}(t)$ versus time for the packet with $k_0 d = 25$.

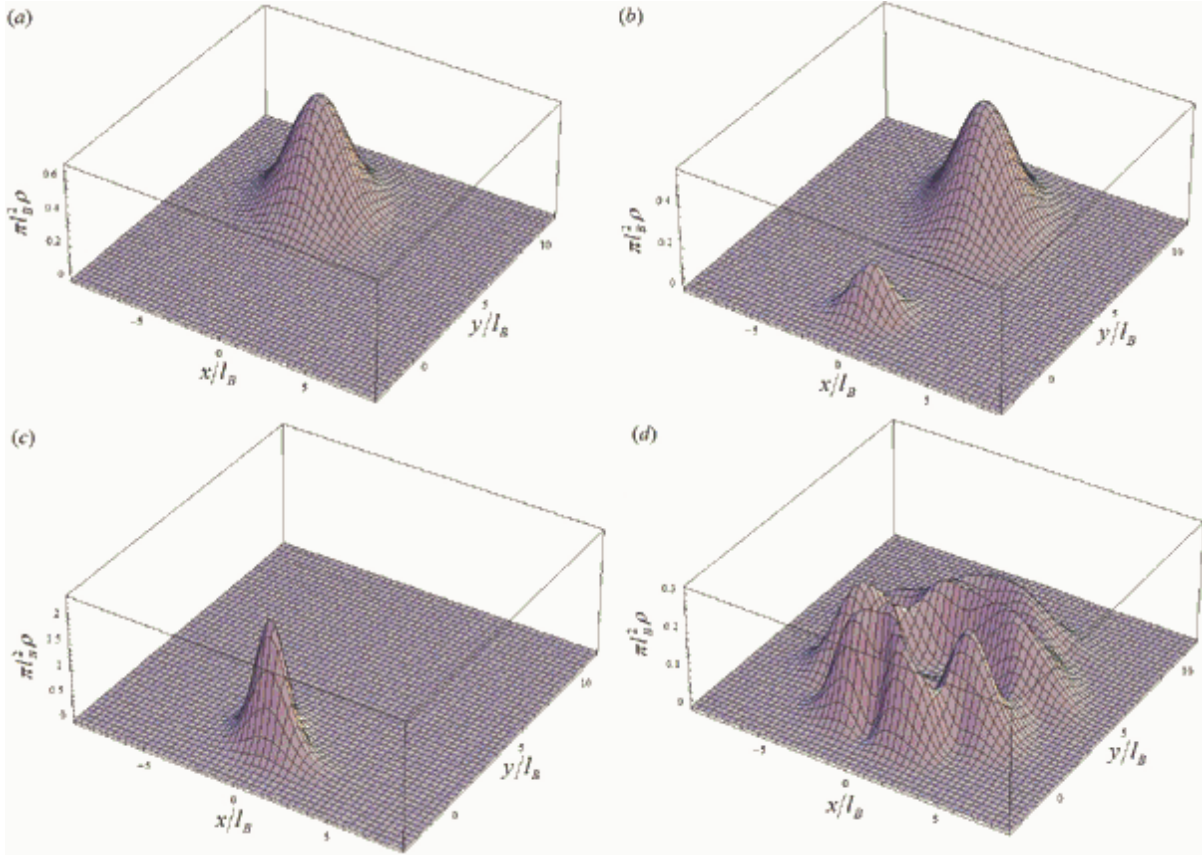


FIG. 5: (Color on line). Evolution of coherent wave packet Eq.(31) in a perpendicular magnetic field: (a) the initial electron density Eq.(31), (b) two split packets at time $t_0 \approx 45 \frac{2\pi}{\omega_c}$, (c) restored packets at time $2t_0 \approx 90 \frac{2\pi}{\omega_c}$, and (d) randomized electron density for large time.

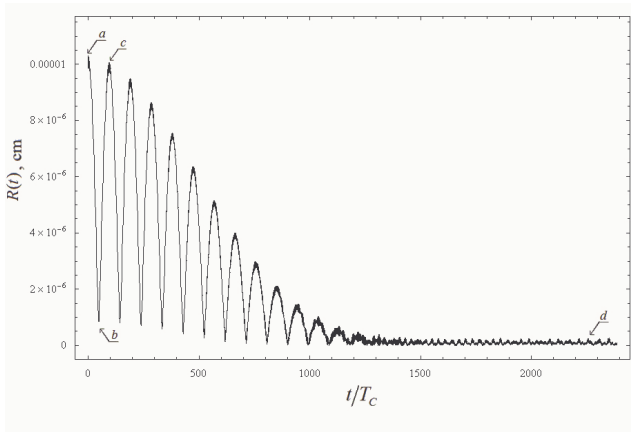


FIG. 6: Cyclotron radius plotted versus the time (for the same parameters as in Fig.5). The distance between maximums and minimums of $R(t)$ marked by arrows is approximately equal to $80T_c$. Time is measured in units of cyclotron period $T_c = \frac{2\pi}{\omega_c}$. The points a , b , c , d correspond to the same moments of time as in Fig.5(a), (b), (c), (d), respectively.